Korea-Australia Rheology Journal
Vol. 19, No. 1, March 2007 pp. 7-16

Dynamic percolation grid Monte Carlo simulation

Nara Altmann, Peter J. Halley and Timothy M. Nicholson*
Centre for High Performance Polymers, Division of Chemical Engineering, University of Queensland QLD 4072, Australia

(Received December 18, 2005; final revision received October 27, 2006)

Abstract

A dynamic Monte Carlo percolation grid simulation is used to predict the cure behaviour of thermoset materials. Molecules are distributed in a fixed grid and a probability of reaction is assigned to each pair of neighbouring units considering both reaction rates and diffusion. The concentration and network characteristics are predicted throughout the whole curing process and compared to experimental data for an epoxy-amine matrix.

Keywords : thermoset curing, Monte Carlo simulation.

1. Introduction

Thermoset resins are used in a range of industrial applications. The broad range occurs due to the possibility of tailoring the final properties of the network by tailoring the formulation of the material. More recently, thermoset materials have become increasingly more important as more complex formulations are being developed. Higher glass transition temperatures and strength, for example, can be obtained through the incorporation of nanoparticles with a high affinity towards the components of the matrix. On the other hand, lower glass transition temperatures and ductibility can be obtained through the incorporation of softer particles such as hyperbranched polymers. A large amount of work has been put into understanding the interactions between the different phases in these composite materials, with the aim of being able to predict the final properties. The effect that different compositions have on the cure kinetics and network formation, however, has largely been neglected. A true understanding of the effect fillers and plasticisers have on the network properties will be aided by an understanding of the network formation process. Furthermore it is desirable to have a model that is able to incorporate the effects of these components on the network development process.

The mechanism of reaction in most thermoset matrices is fairly well understood. The problem, however, is that often this mechanism has been translated into deterministic models, neglecting the fact that the collisions of molecules and their reactions occur essentially in a random manner (Gillespie, 1977). Formulating the rate of reaction in terms of a kinetic rate constant times the bulk concentration of the chemical groups clearly implies that each species experiences the average environment. This may not be the case in multiphase systems and it is not the case in the vicinity of the critical gel point (Dotson *et al.*, 1996). The stochastic nature of the processes becomes increasingly more evident as more complex formulations are used. For such formulations it becomes increasingly more difficult to find deterministic models that will reproduce the experimental data in different circumstances. The use of stochastic models for chemical reactions allows for more complex systems to be modelled in a rather simple way and allow us to easily determine the molecular weight distribution and the molecular structures. The knowledge of these two characteristics is vital to the prediction and understanding of the viscoelastic response of the material and the gelation and vitrification points that are essential in order to be able to optimise the processing of such materials.

Many other authors have presented simulations of the chemorheology during cure. For instance Dubois *et al.* (1998) used a stochastic simulation to determine molecular weight distributions, coupled with the double reptation mixing rule (Cloizeaux, 1992) and Rouse relaxation for short chains to predict the response of linear polyurethanes. This model did not consider non-linear chains, to which the authors attributed discrepancies between the simulated and experimental data at high conversion levels. Prasatya *et al.* (2001) modelled the evolution of residual isotropic stresses in thermosetting materials using a thermo-viscoelastic model which related the characteristic relaxation times to the change in glass transition temperature with conversion. This model was successful in describing the system after the gel point, where such stresses develop, but could not describe pre gel point events. Randrianantoandro *et al.*

*Corresponding author: t.m.nicholson@uq.edu.au

(1996) concentrated their efforts on the response near the gelation point and assumed a power-law distribution of relaxation times.

This paper constitutes the first of a series of two papers, which combines a Monte Carlo percolation grid simulation with a new viscoelastic model to describe the chemorheological behaviour of thermoset materials throughout the curing process. In this paper we describe the dynamic Monte Carlo percolation grid simulation and compare model results with experimental data for an epoxy-amine matrix. The simulation described in this paper gives concentration profiles, molecular weight distributions and distribution of branch sizes. In the second paper, such characteristics serve as input to the viscoelastic model. Since the viscoelastic response is highly sensitive to the characteristics of the network, we analyse how the reaction rate parameters and stoichiometry of the reactants affect the network formation.

2. Dynamic Monte Carlo percolation grid simulation

Molecules are in constant movement due to Brownian motion. When they collide the reaction between reactive functional groups may happen. The overall probability of a reaction occurring is related to both the probability that a collision will occur (related to the diffusion rate) and how to successful such a collision is in producing a reaction (related to the energy of the colliding molecules).

Given that a collision has occurred, a reaction will only result if the energy of the molecules is higher than the activation energy barrier for the reaction event. Molecules follow a Boltzmann type distribution of their energy so that the probability that a collision event will be successful, and therefore the characteristic rate for the reaction, can also be considered to follow a Boltzmann type distribution. The probability of a successful reaction event occurring in a time interval Δt is thus given by

$$P_{react} = 1 - \exp(-k_{avg}\Delta t) \tag{1}$$

where k_{avg} is the average rate of reaction. This approach is taken following a similar approached used by Dawnkaski *et al.* (1995) when modelling the reaction of hydrogen in diamonds.

In the reaction between epoxide and amine groups a number of different reaction paths have been reported. The first one is the direct reaction between amine hydrogen and epoxide forming a hydroxyl group and the carbon-nitrogen bond. The second mechanism involves first the reaction between a hydroxyl group and an epoxide group to form a catalysed complex followed by the reaction of this complex with an amine nitrogen. A number of other reaction paths have also been reported (e.g. see Mijovic *et al.* (1991)), but in this work we have restricted the mechanism to these two and excellent agreement with experimental data has been obtained. Therefore five reaction rates are used in the simulation: for the first reaction pathway the reaction rates for the epoxy group with either a primary (k_1) or a secondary (k_2) amine; for the second pathway the formation of the catalysed complex (k_3) and the reactions of this complex with either a primary (k_4) or a secondary (k_5) amine. At present these constants have been obtained by fitting the simulation results to concentration profiles obtained experimentally, but ultimately they could be obtained from molecular modelling simulations.

The reaction between two functional groups involves not only how effective collisions are, but also to how often these collisions occur, which is related to the diffusion of the groups. There is a probability, P_{diff}, of the molecule having diffused in a time interval Δt to give rise to a collision is given by:

$$P_{diff} = 1 - \exp(-k_{diff}\Delta t) \tag{2}$$

where k_{diff} is the average diffusion rate. The diffusion rate, k_{diff}, is related to the self-diffusion coefficient, D, through the Smoluchwski Equation (Rohr, 1988):

$$k_{diff} = 4\pi d_{ab} A D \tag{3}$$

where d_{ab} is the collision diameter, A is the Avogadro number.

The diffusion coefficient is calculated through the Group Interaction Model of Porter, which for a linear polymer chain of length Z mers (Porter, 1995) is given by:

$$D = \frac{\pi}{2}\frac{L^2}{\tau}\frac{1}{Z^2} \tag{4}$$

where L is the length of a mer unit, and τ is the monomeric relaxation time. This needs to be adapted for branched and cross-linked polymer for use in the case of our epoxy-amine thermoset. Rohr (1988) considered the diffusion of a functional site to correspond to the diffusion of the branch to which it belongs as if the branch was a linear chain, following the work of de Gennes (1971). Essentially, what it means is that for a branch point to react, the centre of mass diffusion of the whole molecule is not required. The time for diffusion is associated with a characteristic relaxation time for the branch and hence to a diffusion coefficient given by the Porter equation with Z the number of mer units in the branch.

The diffusion time for a branch slows down as the reaction progresses because of an overall slowdown in molecular motion as the glass transition temperature, T_g, increases. This is reflected in the monomeric relaxation time τ, given by (Matsuoka, 1992):

$$\tau = \frac{h}{2\pi kT}\left(\exp\frac{E_a}{kT}\right)^z \tag{5}$$

where T is the temperature, E_a is the activation energy for

relaxation, k is Boltzman's constant and h is Plank's constant. z is the cooperativity domain which is given by:

$$z = \frac{T^* - T_{g0}}{T^*} \frac{T}{T - T_{g0}} \tag{6}$$

and accounts for the interference of one segment of chain by other segments of chain near the glass transition temperature. Here T_{g0} is the thermodynamic glass transition temperature which is assumed to be 50°C below the calculated glass transition temperature (Porter, 1995; Gumen *et al.*, 2001). T^* is a high temperature limit which has been suggested to be universal for all polymers and to assume a value of 500°C.

The overall probability of a reaction event occurring, P_{total}, is given by combining the effects of collision energy and diffusion (collision interval):

$$P_{total} = P_{react} P_{diff} \tag{7}$$

The time step used, Δt, should be given by the inverse of the fastest rate of all the existing processes (Dawnkaski *et al.*, 1995). These correspond to each of the kinetic steps in the epoxy-amine mechanism and the diffusion process. We would, however, encounter a problem if we followed this approach. The problem occurs because at the beginning of the reaction, particularly for the higher temperatures, the diffusion rate is several orders of magnitudes higher than the kinetic rates. So if we chose the step rate to be equivalent to the inverse of the diffusion rate, a large number of steps would be required before a reaction would occur and as a result the simulation would become prohibitively slow. As an alternative, we make a simplification and assume the process to be only reaction controlled at the early stages and use a time step of 0.1 times the fastest reaction rate. Simulations using various time steps showed the results to be largely independent of time step for time steps less this chosen value.

3. Algorithm

The simulation was implemented in C and the basic algorithm corresponds to the following steps:

1. Monomers are distributed at random on a cubic grid of pre-defined size with the ratio of epoxy to amine sites corresponding to the desired stoichiometric ratio. Each site in the grid has either an epoxy or an amine molecule with two reactive end-groups each. Periodic boundary conditions are used.
2. One epoxy is selected at random and one of its neighbours chosen, where a neighbour is defined as a molecule that is up to two lattice sites distant. If the neighbour chosen can not possibly react with the epoxy (i.e. it is another epoxy), another neighbour is chosen until either a reactive match is found or eight neighbours have been attempted.
3. Once the epoxy and its neighbour have been chosen the reaction and diffusion probabilities are calculated and hence the combined probability of reaction. Whether or not the reaction will occur is then determined by choosing a random number in the usual fashion.
4. If a reaction has occurred the connectivity between the molecules is set employing a graph theory that avoids the formation of loops (Moukarzel, 1998). The graph theory is described in further detail below where the branching structure is described. The two molecules are set as belonging to the same cluster and cluster size information is updated. This is done using an algorithm presented by Stauffer (Stauffer and Ahrony, 1992), which aids the calculation of cluster sizes by assigning a 'good cluster' label to each cluster. Lattice statistics regarding concentrations are also updated immediately after reaction.
5. Steps 2-4 are repeated a number of times equivalent to the number of epoxies in the simulation. The reaction time is then incremented and the procedure repeated until the reaction achieves a desired final reaction time or final conversion level.

3.1. Branching Structure

As well as the distribution of cluster sizes, the distribution of branch sizes is required for use in the prediction of the viscosoelastic response of the system. This branching structure is obtained using an algorithm developed by Mourkarzel (1998). This assigns the connectivity between molecules in such as way that the connection has a direction and each molecule can have only one connection to it, but may connect on to any number (see Fig. 1). When loops are formed, to aid the branch architecture tracking algorithm, all the molecules that are in the loop are replaced with a single molecule representing the loop. The size of the loop is recorded so that it can be included in the

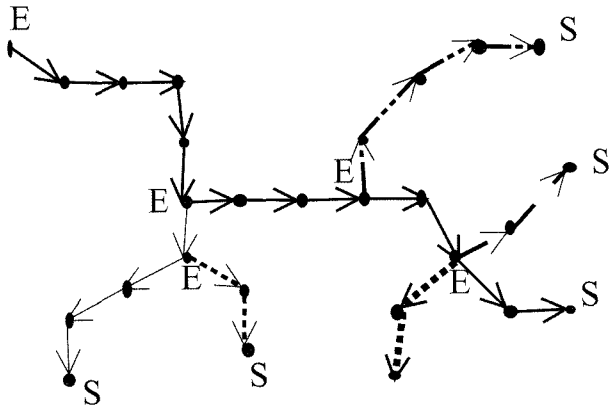

Fig. 1. Representation of sites in the grid and their branches. Sites labelled S correspond to the start of branches and E to the end of btranches in the labelling process

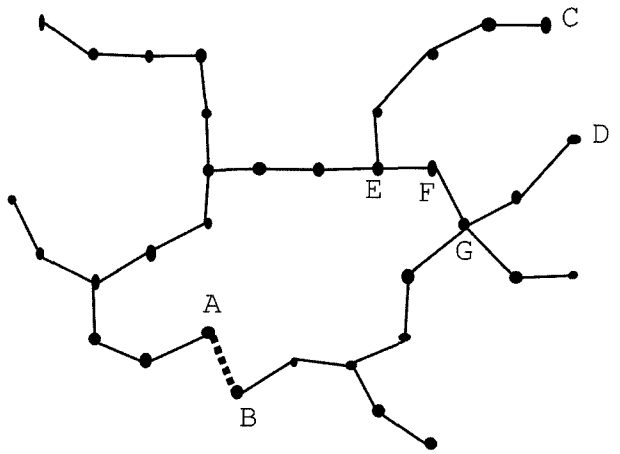

Fig. 2. Representation of a cross-link point. A reaction between molecules A and B will form a cross-link.

calculation of the branch size.

Cross-linking occurs when sites already belonging to the same molecule join each other. A representation of the formation of a cross-link is shown in Fig. 2 when sites A and B join each other. There is a difference, however, between elastically active cross-links and loops. Elastically active cross-links are those that are connected to the network structure through more than one junction point. If one follows the connections between the molecules from B, there is only one path that leads back to A and a loop is formed. If however points C and D are connected, then it is possible to reach A going through C and D as well as via the original path so the crosslink structure becomes an active crosslink. One is able to identify the formation of an active crosslink structure when a loop is formed that include molecules that are already in a loop (molecules E, F and G in Fig. 2) and hence flag the loop as an active cross-link.

At regular time intervals during the simulation the branching structure data are updated. Each molecule in the grid is checked. A molecule which has no connection out of it corresponds to the end of a branch (molecules labelled S in Fig. 1) and the connections from such a molecule are followed backwards, labelling the transversed molecules as belonging to the same branch until either an already labelled molecule, the end of the branch (a molecule with more than one forward link such as labelled E in Fig. 1), or an effective cross-link site is reached. In this way we are able to map the structure of the branches in each polymeric chain.

Through this algorithm it is also possible to obtain two other characteristics of the non-linear chains. These are the distribution of end sizes and the distribution of loop sizes. Ends correspond to branches up to a junction point, which are linear chain segments.

For each chain we group the branches, ends and loop sizes in regular logarithmic intervals of their sizes. The longest branch of a molecule is considered to be the backbone of the molecule.

3.2. Gelation and vitrification

Gelation is considered to occur when a percolating cluster is formed (Stauffer *et al.*, 1982). By percolating cluster we understand a cluster that spans over the entire lattice in all three dimensions. This is determined by recording the maximum and minimum coordinate of each cluster. When the difference between these (in each dimension, and taking into account periodic boundary conditions) exceeds the lattice size for one cluster gelation is assumed to have occurred.

Vitrification occurs when the glass transition temperature for the system surpasses the cure temperature. This is determined in the simulation in two ways. As the vitrification point is approached the diffusion rate falls, and the start of vitrification is taken to be when P_{diff} is less than 0.9, i.e. the diffusion rate is approaching the reciprocal of the time step (which is related to the inverse of the reaction rate). Alternatively, the glass transition temperature can be calculated as described below and used directly.

4. Results and discussion

The model was calibrated and verified using an epoxy-amine thermoset system composed of the diafunctional diglycidylether bisphenol-F (DGEBF) and the tetrafunctional methylenedianiline (DMA).

4.1. Concentration profiles and glass transition temperature

These data were used to fit the parameters needed in the simulation: the rate constants, and the change in degrees of freedom with changing topology.

Fig. 3 compares the model results for concentration profiles of epoxide, primary and secondary amines with experimental data for a range of cure temperatures. The experimental profiles were obtained using FTIR spectroscopy, with the primary amine concentration being determined from the 5056 cm^{-1} band, the secondary amine from the 6670 cm^{-1} band (subtracting the primary amine concentration) and the epoxide concentration from the 4530 cm^{-1} band (Mijovic and Andjelic, 1995) The excellent fit shown in these graphs is due to these data being used to obtain the rate constants via a genetic algorithm. A grid size of 40^3 was used for these fits; a larger grid size did not change the fitted parameters, but substantially increased the time for the algorithm to run. The fit was more sensitive to changes in the values of rates for the catalysed reaction (k_3, k_4 and k_5) than for the direct reaction (k_1 and k_2) as the latter occurs an order of magnitude slower. As expected the fit for the epoxide was sensitive to the rate of formation of the catalysed complex (k_3), whilst the fit for

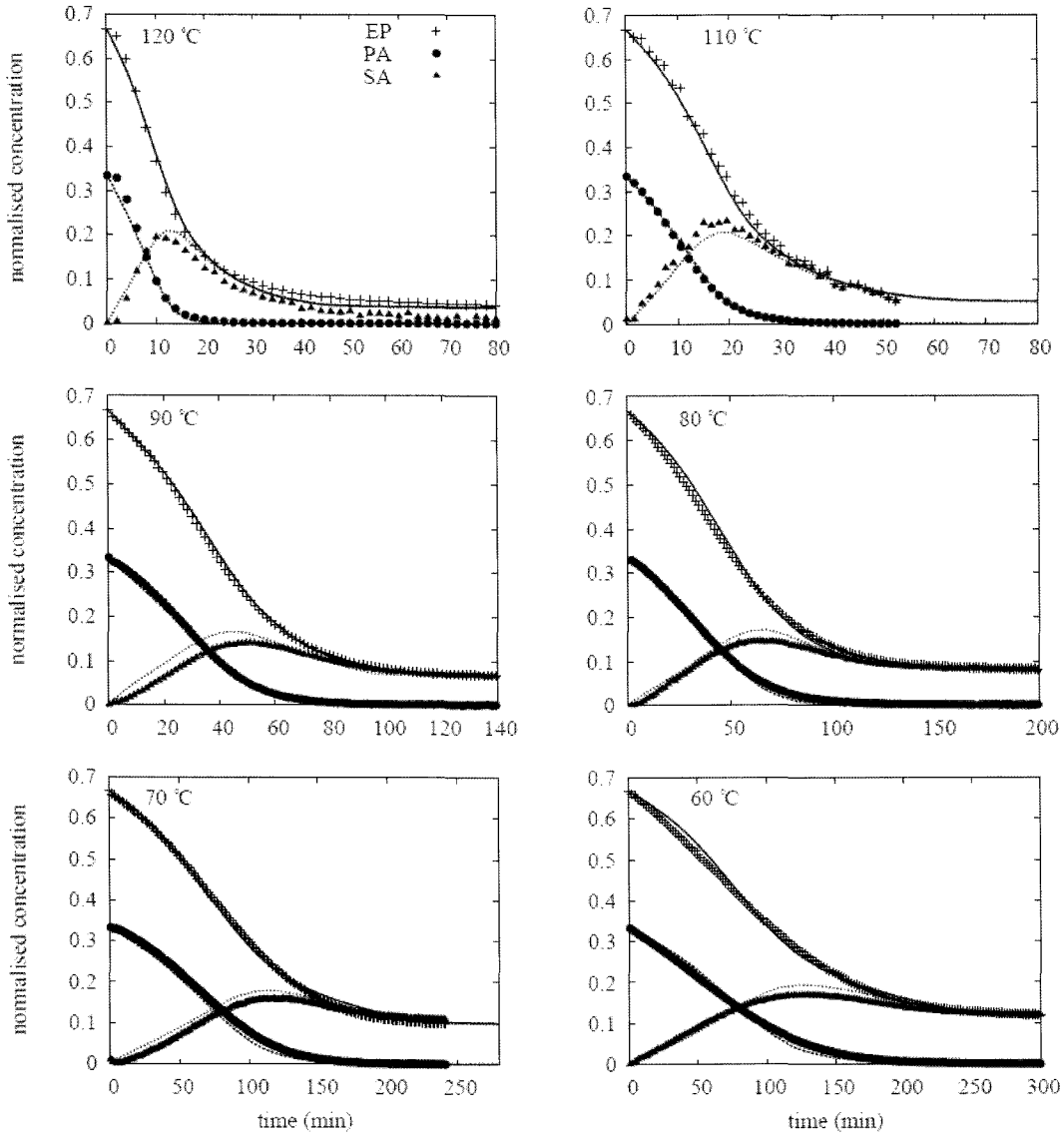

Fig. 3. Best fits of model to experimental concentration profiles. Dots are experimental data and lines the model fit.

the secondary amine was most sensitive to the rate of reactions of the complex with primary and secondary amines.

The kinetic rates follow an Arrhenius relationship with temperature as shown in Fig. 4, from which activation energies for the processes can be deduced (see Table 1). These activation energies are lower than the literature values (Moroni *et al.*, 1986; de Miranda *et al.*, 1997) and together with the absence of an initial plateau in the epoxide concentration which is typical of auto-catalytic reactions (Smith, 1961) suggests that the rate of the non-catalysed reaction is similar to the catalysed reaction initially. As the non-catalysed reaction would be expected to be slower at first, sources of hydroxyl groups other than those considered in the simulation are probably present in the experimental sample. Despite this, the percolation model seems to be able to model the reaction well, in particular accounting for the slow down in the reaction rates due to diffusion effects.

Table 1. Activation energies and pre-exponential factors for the epoxy-amine reactions from Fig. 4.

k	Reaction	k_0	E_a
k_1	EP+PA	$7{:}88\times10^{2}$	44.2
k_2	EP+SA	$6{:}83\times10^{-3}$	6.9
k_3	EP+OH	$7{:}37\times10^{3}$	45.9
k_4	EPcat+PA	$1{:}05\times10^{4}$	45.4
k_5	EPcat+SA	$1{:}13\times10^{4}$	49.7

The glass transition temperature as a function of cure was measured using modulated differential scanning cal-

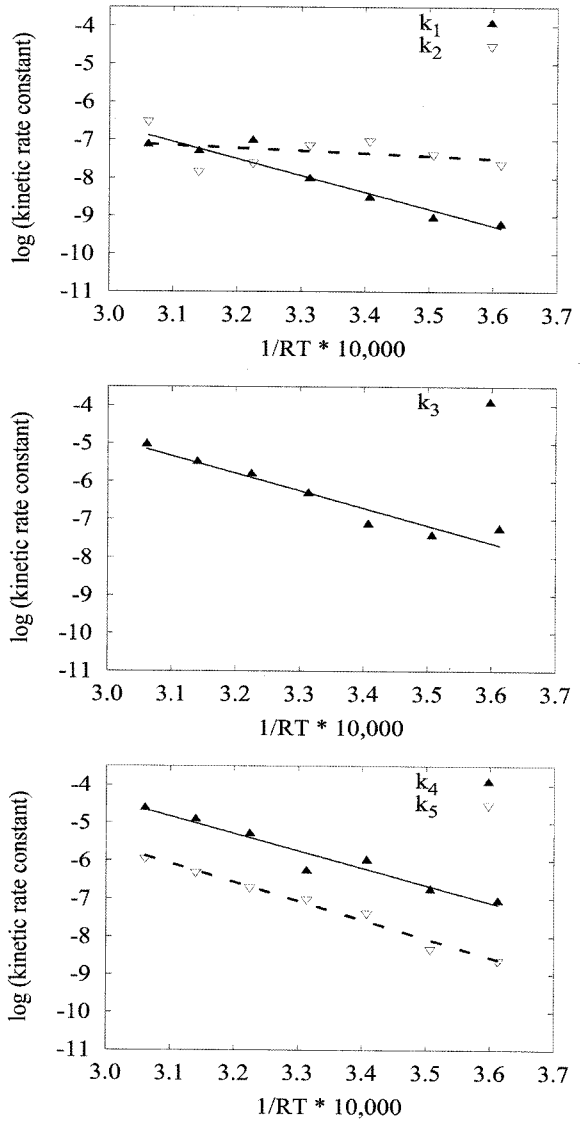

Fig. 4. Arrhenius fit to the kinetic rate constants ontained from the best fit of the model to the experimental data

orimetry. Samples at different cure times were cooled down to −20°C at 20°C/min and then a scan performed heating at 5°C/min from −20°C to 180°C. The glass transition was taken as the midpoint in the step increase of heat capacity.

This was compared to the glass transition temperature calculated using the Group Interaction Model, which requires the number of degrees of freedom per mer unit (N_c):

$$T_g = 0.224\,\theta_1 + 0.0513\frac{E_{coh}}{N_c} \tag{8}$$

where E_{coh} is the cohesive energy and θ_1 a reference temperature characterising the vibrations in the chain axis (Porter, 1995). E_{coh} is obtained from tabulated values given by Porter. The number of degrees of freedom depends on

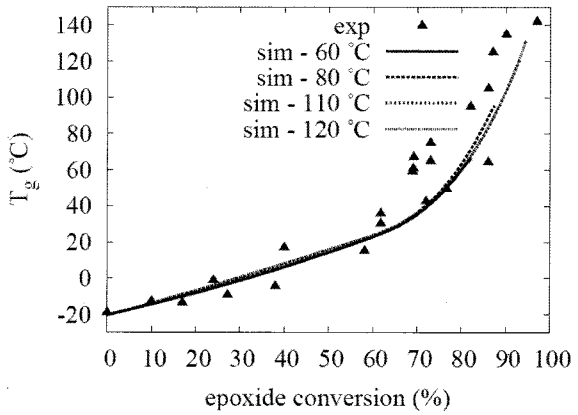

Fig. 5. Glass transition temperature as a function of conversion. Comparison between experimental and simulation results.

the chain topology. The number of degrees of freedom per mer unit and the extra degrees of freedom for a chain end are given by Porter. Cross linking decreases the number of degrees of freedom and this number lost per cross-link (N_{cross}), together with the reference temperature θ_1 are fitted from the experimental data. The results are shown in Fig. 5, where again good agreement is apparent because these data have been used to fit simulation parameters. The number of degrees of freedom decreases more strongly and the glass transition temperature increases strongly after gelation when cross-linking starts to occur more frequently.

4.2. Gelation, vitrification and the TTT diagram

Experimental gelation and vitrification points were determined on a Rheometrics RDS II rheometer using a parallel plate geometry and multiwave frequency time sweeps. The gelation point was taken as the crossover in the loss tangent (Winter and Chambon, 1986) and the vitrification as the peak in the loss tangent at $\omega = 2\pi\ s^{-1}$ (Lange *et al.*, 2000).

The simulation prediction for gelation and vitrification is compared with experimental data in Fig. 6, using the definition of gelation and the two measures of vitrification given above. This is a time-temperature-transformation (TTT) diagram. At higher temperatures the experimental and simulation gelation points agree well, though at 60°C the experimental gelation time is more than twice the simulated one. A possible explanation of this comes from considering the first of the two simulation vitrification lines (which corresponds to the diffusion rate approaching the reciprocal of the simulation step). It is seen that diffusion limitations start to occur before the gelation point and suggests that vitrification effects are affecting the experimental determination of the gel point. The second simulation vitrification curve (corresponding to the point where T_g surpasses the cure temperature) agrees quite well with the experimental values.

An alternative way of representing these data is to plot a Conversion Temperature Transformation (CTT) diagram as

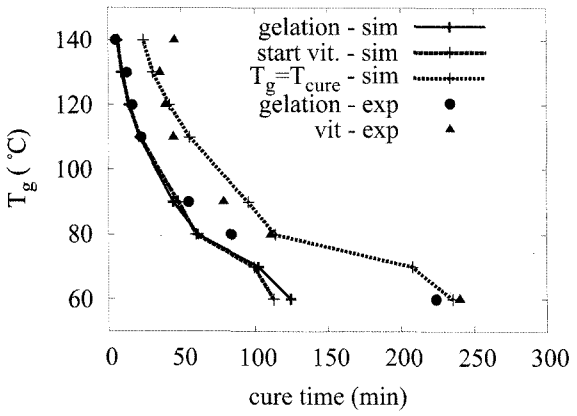

Fig. 6. TTT diagram. Comparison between gelation and vitrification times predicted from the simulation with values obtained experimentally.

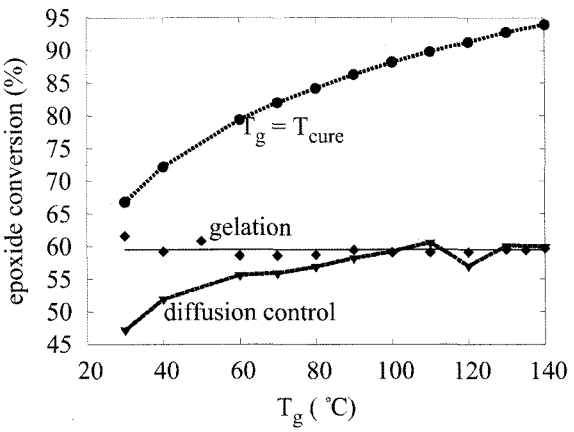

Fig. 7. CTT diagram. Comparison between gelation and vitrification times predicted from the simulation and obtained experimentally.

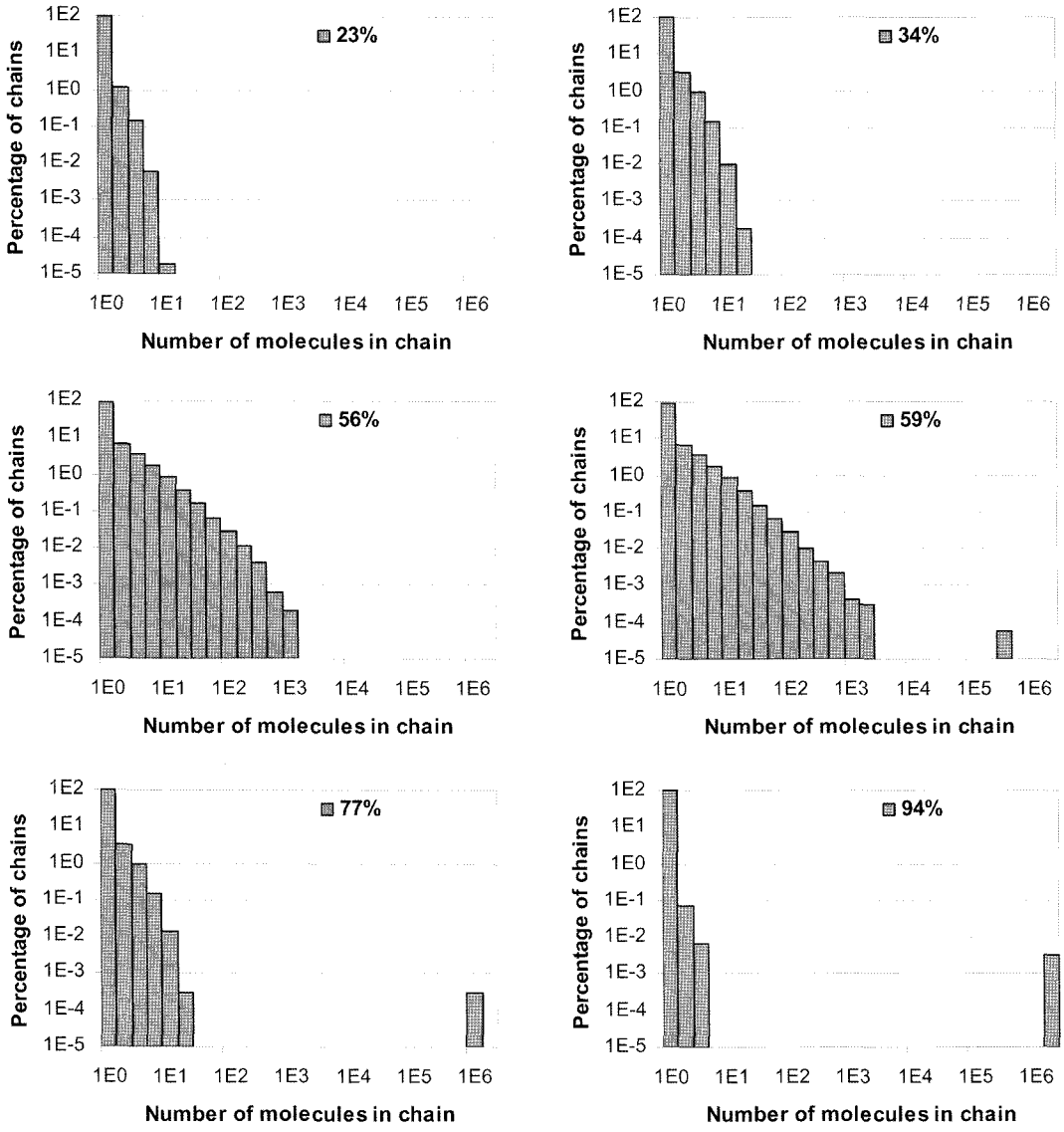

Fig. 8. Distribution of cluster sizes during isothermal cure at 120°C. Gelation corresponds to 59% conversion.

shown in Fig. 7. Here, rather than using the fitted values for the rate constants for each experimental temperature (as in the previous results), the Arrhenius parameters (calculated from Fig. 4) have been used to generate the required rate constants. It is seen that gelation occurs at the same conversion point at all cure temperatures. This conversion value (59.4%) is slightly higher than the Flory-Stockmayer prediction of 57.7% (Stockmayer, 1943; Flory, 1953) and slightly lower than the 61.8% reported by Riccardi and Williams (1993).

As the temperature is decreased the reaction is affected by diffusion limitations at conversions below that of the gel point, so smaller segments will react preferentially to larger ones and give rise to different structures and hence differing rheological behaviours to those produced at higher cure temperatures.

4.3. Molecular weight and branch size distributions

The simulation procedure can additionally give structural information such as the distribution of molecular weights and branch sizes. These data can be used to predict the rheological properties of the system, as described in the second paper in this series.

Fig. 8 shows the distribution of molecular weights of clusters at conversions of 23%, 37%, 51% 59.5% (the gelation point), 73% and 93% for simulations run at 120°C on a grid of size 200^3. Up to the gel point a power law distribution is seen as predicted by other models (Martin *et al.*, 1989; Dotson *et al.*, 1996; Randrianantoandro *et al.*, 1996). The cut off point in this power-law distribution increases up to the gel point where the distribution should stretch to infinity were it not for the finite size of the simulation. Beyond the gel point the cut-off in molecular weight distribution falls to lower values as clusters join the gelled cluster as it continues to grow. The calculated gel point and time were compared for different grid sizes ranging from 20^3 to 200^3 (8k to 8M points) and these showed constant values for grid sizes above 60^3.

Fig. 9 shows a comparison between the predictions for the molecular weight distribution for four different grid sizes ranging from 60^3 to 200^3. The molecular weight distribution below the gel point and the distribution in the sol fraction above the gel point are consistent with only the size of the gelled cluster varying with simulation size (the right-hand point in parts (B) and (C) of this figure correspond to the single gelled cluster). The mean cluster size increases with conversion up to the gel point and then decreases above this. It is to be expected that where this mean size is less than the size of the simulation grid the finite size of the grid will have no effect on the results and so only very close to the gel point will deviations due to the simulation size be noticeable, and then only the high molecular weight tail will differ.

Fig. 10 shows the weight and number average molecular

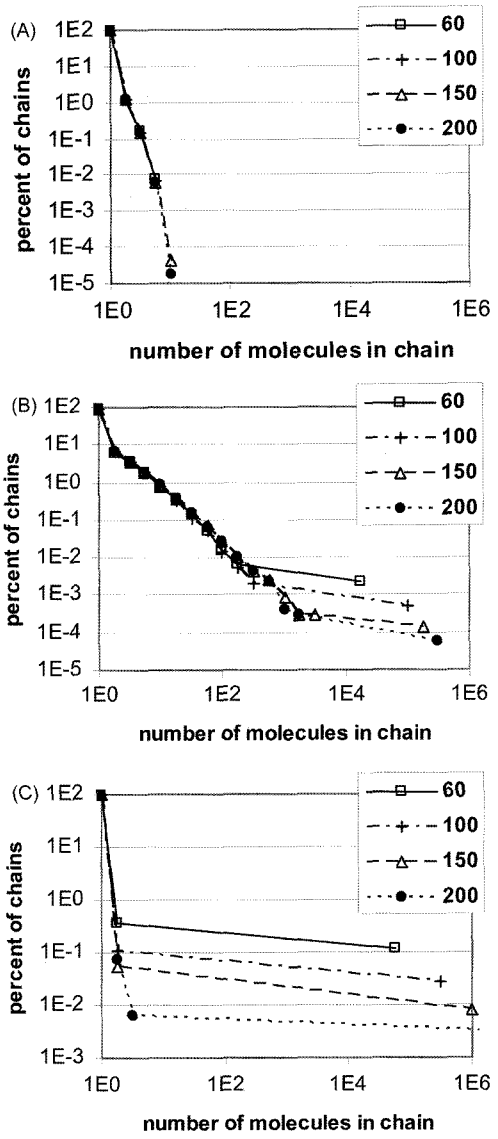

Fig. 9. Comparison between molecular weight predictions for four different grid sizes at (A) 22% conversion, (B) 59% conversion (gel point) and (C) 94% conversion.

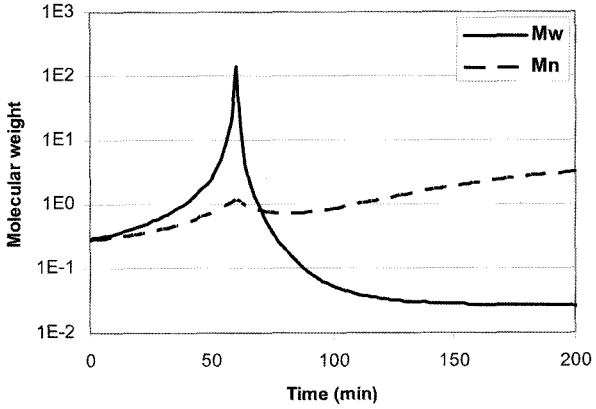

Fig. 10. Number (M_n) and weight average (M_w) molecular weights of the sol fraction during isothermal cure at 120°C.

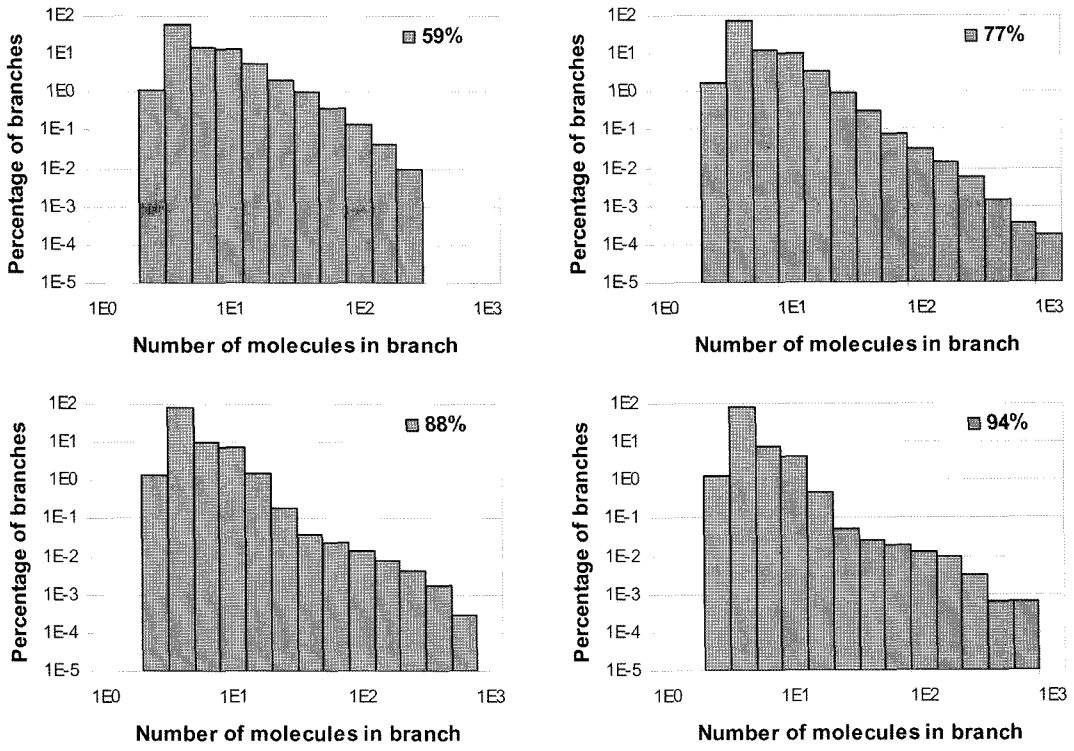

Fig. 11. Distribution of branch sizes at various points in isothermal cure at 120°C.

weights of the sol fraction throughout the cure process at 120°C. Both increase up to gelation at which point the gelled cluster is removed from the calculation and the molecular weights drop. After gelation the weight average molecular weight (M_w, which corresponds to the average cluster size a mer unit is in) decreases continually as larger clusters join the gelled clusters preferentially to smaller clusters. The number average molecular weight (M_n, corresponding to the mean size of clusters in the sol fraction) decreases at first and then increases as small clusters aggregate.

Fig. 11 shows the distribution of branch sizes within the gel cluster immediately after gelation and at three higher conversion levels. These show a power-law distribution of branch sizes within the gel cluster. Branch distributions cannot be measured experimentally, but these data are used as an input to the chemorheological model described in the second paper in this series to obtain data that compares well to the experimental characterisation of the cure process including the power law relaxation spectra at gelation. These results suggest that the molecular weight and branch size distributions calculated by this model are indeed representative of the real system.

5. Conclusion

In summary, we can calculate the network characteristics of a curing thermoset material throughout the whole cure process using a dynamic percolation grid Monte Carlo simulation. The network characteristics that may be calculated are the following:

- concentration of (reactive) chemical groups
- molecular weight distribution, as well as number and weight average molecular weight
- distribution of branch and loop sizes
- number of cross-links, and concentration of elastic chains
- glass transition temperature

We are able to obtain all the above information based only on the reaction rates of each of the reaction mechanism and the diffusion rate. Ideally, the reaction rates could be calculated from quantum mechanics or molecular dynamics simulations. so that the model may be used for prediction of the network development without the need of experimental data. In the second paper of this series we describe the viscoelastic model and how the information generated by the Monte Carlo simulation is used to predict the viscoelastic behaviour of thermosets during cure.

References

Cloizeaux, J. D., 1992, Relaxation of entangled and partially entangled polymers in melts-time-dependent reptation, *Macromolecules* **25**, 835-841.

Dawnkaski, E. J., *et al.*, 1995, Time-dependent monte-carlo simulations of radical densities and distributions on the diamond

(001)(2x1)/H surface, *Chemical Physics Letters* **232**, 524-530.

de Gennes, P. G., 1971, Reptation of a polymer chain in the presence of fixed obstacles, *Journal of Chemical Physics* **55**, 572-579.

de Miranda, M. I. G., *et al.*, 1997, A DSC kinetic study on the effect of filler concentration on crosslinking of diglycidylether of bisphenol-A with 4,4'-diaminodiphenyl methane, *Polymer* **38**, 1017-1020.

Dotson, N. A., *et al.*, 1996, Polymerization Process Modeling VCH Publishers, New York.

Dubois, C., *et al.*, 1998, Chemorheology of polyurethane systems as predicted from Monte Carlo simulations of their evolutive molecular weight distribution, *Journal of Rheology* **42**, 435-452.

Flory, P. J., 1953, Principles of polymer chemistry Cornell University Press. Ithica, New York.

Gillespie, D. T., 1977, Exact stochastic simulation of coupled chemical-reactions, *Journal of Physical Chemistry* **81**, 2340-2361.

Gumen, V. R., *et al.*, 2001, Prediction of the glass transition temperatures for epoxy resins and blends using group interaction modelling, *Polymer* **42**, 5717-5725.

Lange, J., *et al.*, 2000, Understanding vitrification during cure of epoxy resins using dynamic scanning calorimetry and rheological techniques, *Polymer* **41**, 5949-5955.

Martin, J. E., *et al.*, 1989, Viscoelasticity near the sol-gel transition, *Physical Review A* **39**, 1325-1332.

Matsuoka, S., 1992, Relaxation Phenomena in Polymers Hansen, New York.

Mijovic, J. and S. Andjelic, 1995, A study of reaction-kinetics by near-infrared spectroscopy. 1. comprehensive analysis of a model epoxy/amine system, *Macromolecules* **28**, 2787-2796.

Mijovic, J., *et al.*, 1991, Mechanistic modeling of epoxy amine reactions, *Abstracts of Papers of the American Chemical Society* **202**, 162.

Moroni, A., *et al.*, 1986, Cure Kinetics of epoxy-resins and aromatic diamines, *Journal of Applied Polymer Science* **32**, 3761-3773.

Moukarzel, C., 1998, A fast algorithm for backbones, *International Journal of Modern Physics C*, **9**, 887-895.

Porter, D., 1995, Group interaction modelling of polymer properties Marcel Dekker, New York.

Prasatya, P., *et al.*, 2001, A viscoelastic model for predicting isotropic residual stresses in thermosetting materials: Effects of processing parameters, *Journal of Composite Materials*, **35**, 826-848.

Randrianantoandro, H., *et al.*, 1996, Slow dynamics in gels, *Journal of Non-Newtonian Fluid Mechanics* **67**, 311-323.

Riccardi, C. C. and R. J. J. Williams, 1993, Modeling strategy for systems with both stepwise and chainwise chemistry revisited - the directionality effect on the buildup of the Network structure, *Journal of Polymer Science Part B-Polymer Physics* **31**, 389-393.

Rohr, D. F. J., 1988. Modelling reaction and diffusion in epoxy-amine polymerization kinetics. Delaware, University of Delaware.

Smith, I. T., 1961, The mechanism of the crosslinking of epoxide resins by amines, *Polymer* **2**, 1357.

Stauffer, D. and A. Ahrony, 1992, Introduction to Percolation Theory Taylor and Francis, London.

Stauffer, D., *et al.*, 1982, Gelation and critical phenomena, *Advances in Polymer Science* **44**, 103-158.

Stockmayer, W. H., 1943, Theory of molecular size distribution and gel formation in branched-chain polymers, *Journal of Chemical Physics* **11**, 45-55.

Winter, H. H. and F. Chambon, 1986, Analysis of linear viscoelasticity of a cross-linking polymer at the gel point, *Journal of Rheology* **30**, 367-382.